Vibration Injury Network

Research Network on Detection and Prevention of Injuries due to Occupational Vibration Exposures

A comparison of two methods of simulating the dynamic response of suspension seating

Appendix W4C to Final Report
May 2001

EC Biomed II concerted action BMH4-CT98-3291

T. Gunston, J. Rebelle* and M. Griffin

Institute of Sound and Vibration Research, University of Southampton, England
**Institut National de Recherche et de Sécurité, Nancy, France*

1 Introduction

Theoretical models of suspension seats allow seat behaviour to be investigated without laboratory testing and without exposing human subjects to the high levels of vibration typical of suspension seat operating conditions. Various non-linear theoretical models of suspension seats have been described (e.g. Rakheja *et al.,* 1987, Gouw *et al.*, 1990, Rakheja *et al.*, 1994; Ranganathan and Sriram 1994; Wu and Griffin, 1995; Ahmed and Goupillon, 1997; Tewari and Prasad, 1999; Gunston, 2000; Rebelle, 2000). The majority of these models have used a lumped-parameter approach to describe the seat in terms of coefficients related to specific component parts and then solved the resulting non-linear equations using numerical integration techniques. The complexity of suspension seat models has progressively increased by including more detailed descriptions of the seat component parameters. The ISVR model, as described by Gunston (2000), continues this approach.

An INRS model, described by Rebelle (2000), adopted an alternative approach. The seat suspension and cushion were described using a Bouc-Wen model (Bouc, 1967; Baber and Wen, 1981) rather than in terms of specific coefficients for the individual components. The coefficients describing the seat dynamic behaviour were determined by curve-fitting to the measured behaviour of a specific seat. This approach allows a set of parameters to be determined quickly for an existing seat from a small number of laboratory measurements, rather than by measuring each component individually.

This study tested two suspension seats in the laboratory and compared the measured seat performance with predictions made by the two alternative suspension seat models from ISVR and INRS. The models tested were the discrete parameter model developed at the Institute of Sound and Vibration Research (as described by Gunston, 2000) and the Bouc-Wen model developed at the Institut National de Recherche et de Sécurité (as described by Rebelle, 2000). The ISVR model was tested using measured damper coefficients and using an alternative set of coefficients optimised to the measured seat performance. The intention was to identify strengths and weaknesses of the alternative models.

2 The seats

Two production suspension seats were used for this investigation. The first was a compact design for use in industrial trucks with the suspension components mounted behind the backrest (Figure 1). The second seat was a model used in earthmoving machinery and had the suspension components mounted under the seat cushion (Figure 2). Both seats used covered foam cushions, steel coil springs, oil dampers and rubber end-stop buffers.

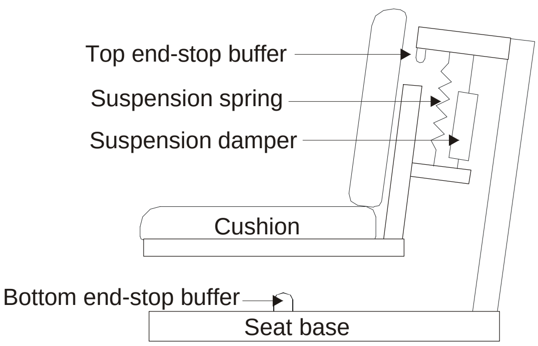

Figure 1 Schematic of the industrial truck seat

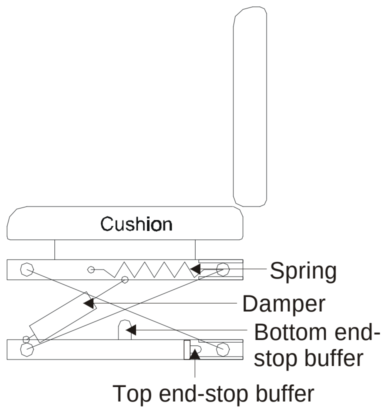

Figure 2 Schematic of the earthmover seat

3 The models

3.1 The INRS model

3.1.1 Seat suspension model – Assumptions

To limit the number of parameters needed to model the behaviour of the seat, a global approach was considered, based on the measurement of the input motion (acceleration, relative velocity or relative displacement) and output motion (acceleration, relative velocity or relative displacement) recorded, respectively, at the seat base and on the seat cushion.

Figure 3 shows a typical hysteretic behaviour of the seat measured with random excitation in a frequency range including the seat resonance frequency.

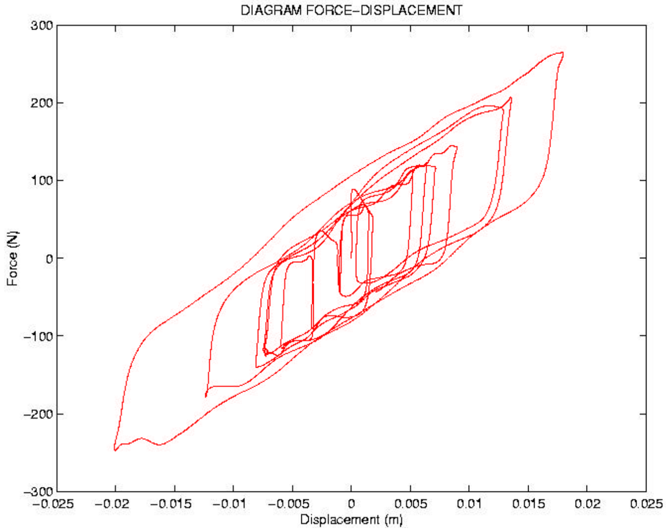

Figure 3: Force-displacement diagram - Seat exposed to random excitation.

The Bouc-Wen model describes a wide variety of hysteretic systems (Bouc, 1967). The friction force $Z(t)$ is related to the relative displacement $u(t)$ of the suspension according to the first order non-linear differential equation:

$$\dot{Z}(t) = (K - K_s)\dot{u} - g\,|\dot{u}|Z - b\,\dot{u}\,|Z| \tag{1}$$

where K and K_s are positive stiffnesses and where g and b give the effect of the hysteresis. This model was first proposed by Bouc in 1967, then generalised and applied to structures under earthquake excitation by (Wen, 1976; Baber and Wen, 1981) and has been widely used for other applications since.

A non-linear single-degree-of-freedom vertical seat suspension with hysteresis can be modelled by two equations as follows:

$$\begin{cases} M\ddot{u} + C\dot{u} + K_s u + Z + F_T + F_B = -M\ddot{y} \\ \dot{Z} = (K - K_s)\dot{u} - g\,|\dot{u}|Z - b\dot{u}|Z| \end{cases} \tag{2}$$

where $u(t)$ is the vertical relative displacement of the suspension, $Z(t)$ is the previously defined Bouc-Wen force, M is the mass, C is the viscous damping coefficient (assumed to be linear), K_s is the stiffness of the suspension, and $\ddot{y}(t)$ is the input excitation. F_T and F_B represent the reaction force of the end-stop top buffers (F_T - Equation 3) and the bottom end-stop buffers (F_B - Equation 4). All the non-linear effects due to the different seat components are combined in the force, $Z(t)$. Mass M $(= m_i + m_{mp})$ represents the inert mass placed on the cushion (m_i) and the mass of the moving parts of the seat suspension (m_{mp}), both masses are assumed to be rigidly fixed to the seat suspension. Consequently, five parameters must be identified to describe the suspension behaviour (with no impact on the buffers) : C, K_s, K, g and b.

The top end-stop buffers were modelled simply as an equivalent buffer (i.e. a soft linear spring-damper, $C_T;K_T$, system) which produces a reaction force, F_T, when the suspension exceeds its mid free-travel (d). The relative motion between the inert mass and the seat cushion were neglected. The inert mass was considered as fixed to the seat suspension model. On the other hand, this relative displacement was taken into account in the top buffer model to describe the acceleration time histories measured on the mass (see Section 3.1.2.2.2).

$$F_T = K_T(u-d) + C_T\dot{u} \qquad u > d \tag{3}$$

The bottom buffers were modelled as a cubic non-linear stiffness ($K_B;K_{B1}$):

$$F_B = K_B(u+d) + K_{B1}(u+d)^3 \qquad u < -d \tag{4}$$

In the model, F_T and F_B represent the reaction force of each end-stop buffer of the seat.

3.1.2 Identification of the parameters

The parameters of the whole seat model were identified in two steps. Firstly, the suspension model parameters were obtained by means of curve fitting using the output acceleration time histories measured with no end-stop impacts. Secondly, the end-stop model parameters were also identified by curve fitting using the static force-deflection curves for the bottom buffer and using output acceleration measurements for the equivalent top buffer.

3.1.2.1 Identification of the seat suspension model parameters

The test seats were mounted on a hydraulic shaker platform and excited by imposed random displacement signals over a frequency range from 0.5 Hz to 5 Hz. The excitation was generated during 16 seconds and included high and low levels of displacement amplitudes in order to generate all the seat behaviour phases: stick-slip phases and free motion. The absolute input acceleration was measured on the shaker platform. The relative output displacement and the absolute acceleration of the seat were also measured. Data acquisitions started with a zero level, for a few seconds, to fulfil null initial conditions in the numerical integration of the dynamic equations. The forklift seat was loaded with a 45 kg mass and the earthmover seat with a 58 kg mass (m_i). The mass of the moving part of the seat was estimated at about 13.5 kg and 27 kg respectively (m_{mp}). The total moving mass, M, was therefore equal to 58.5 kg and 85 kg.

The identification procedure was based on an optimisation method (SIMPLEX method, Nelder and Mead, 1965; or Levenberg-Marquardt method, Moré, 1977) minimising the quadratic error between the measurement and the numerical solution. The latter was obtained by the fourth-order Runge-Kutta method. The parameter values obtained are given in Table 1:

Table 1: Calculated parameter values of the seat suspension.

	K_s (N/m)	K (N/m)	g (m^{-1})	b (m^{-1})	C (Ns/m)
Forklift	8156	320897	94371	-83727	301.3
Earthmover	5420	146620	87270	-84660	507

An example of the fit obtained from this calculation is shown in Figure 4:

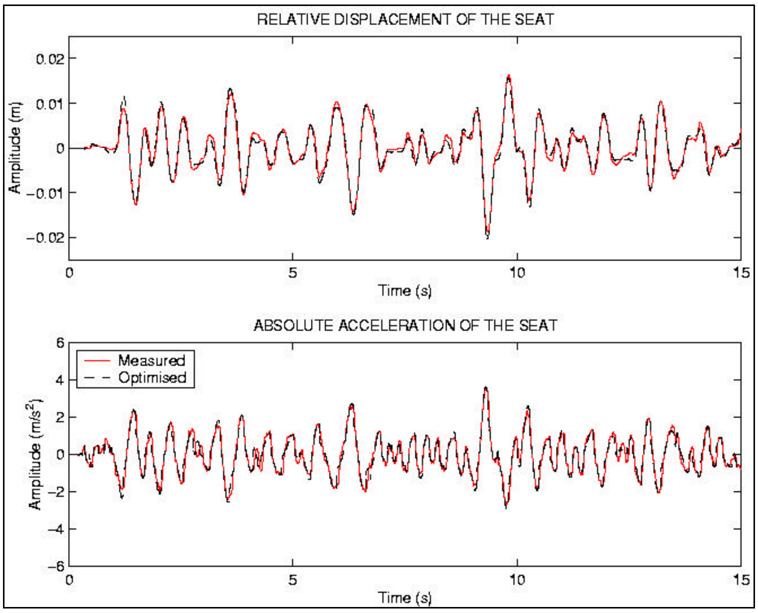

Figure 4: Comparison between the calculated and measured output time histories. Seat loaded with a 45 kg mass (m_i).

The main advantage of this approach is the simplicity of its application. In fact, to model any seat behaviour governed by the model defined in Equation 2 (not including impacts), the methodology required only two accelerometers: one for the input the other for the output. Moreover, this was achieved without dismantling the suspension components.

3.1.2.2 Identification of the end-stop model parameters

3.1.2.2.1 Bottom buffer

The dynamic effects on the nominal bottom buffers were neglected. The end-stop buffers were modelled as a pure non-linear stiffness. The static force-deflection curve of the bottom buffers shown in Figure 5 was used to identify, by curve fitting, the model parameters given in equation (4): K_B and K_{B1}.

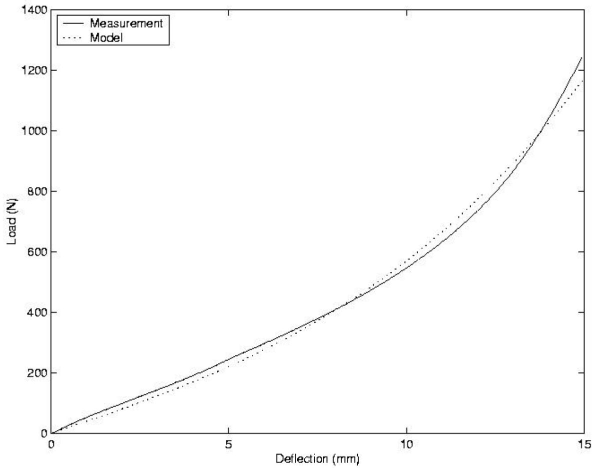

Figure 5: Comparison between modelled and measured buffer force-deflection curves.

The values of K_B and K_{B1} are reported in Table 2.

3.1.2.2.2 Top buffer

The aim was not to describe the real behaviour of the top buffers but to predict the amplitude of output acceleration peaks correctly when top impacts occur. Consequently, the relative displacement of the mass during the impact phases was not well described because the mass was considered as fixed to the seat. In practice, during high impacts, the mass is not always in contact with the seat cushion. The parameters of the impact force, F_T, were identified by fitting the whole model to the output acceleration response when impacts occurred. During this identification, all the seat parameters, including those of the bottom buffers, were kept at their previously identified values. Top buffer parameter values, C_T and K_T, were optimised from Equation 2. Table 2 gives the calculated values of the top and bottom buffer parameters.

Table 2: Parameter values of top and bottom buffer models (equation (3) and (4)).

	K_B (N/m)	K_{B1} (N/m^3)	C_T (Ns/m)	K_T (N/m)
Forklift	80000	3.4E8	200	9000
Earthmover	25020	1.46E8	0	6000

From the calculated result, the top buffers appeared to be soft, whereas their physical behaviour was experimentally found to be relatively stiff (in the static force-deflection curve). This result arises because the relative displacement between the inert mass and the seat cushion was neglected in the seat suspension system but was taken into account within an equivalent top buffer model.

For details concerning the validation of the model, referred to (Rebelle, 2000).

3.2 The ISVR model

3.2.1 Model structure

The ISVR model is shown schematically in Figure 6. The equations describing each component can be found in Gunston (2000). The equations were solved by numerical integration using a 4^{th} order Runga-Kutta algorithm.

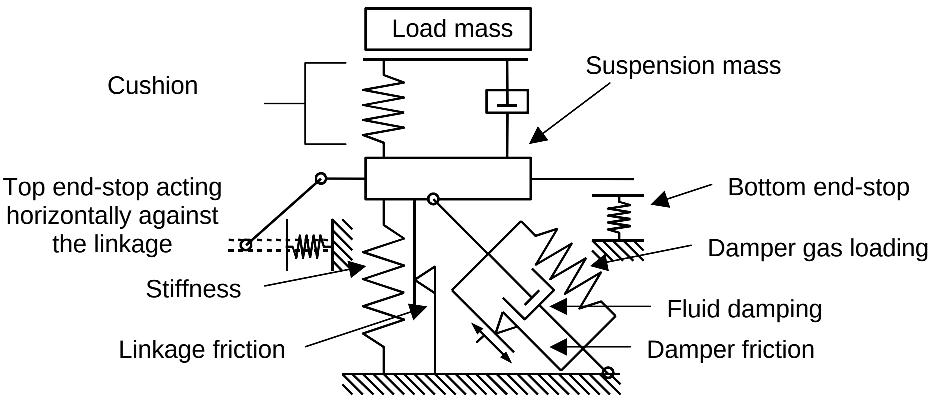

Figure 6 Schematic of the ISVR mathematical model.

The cushion was described by a linear spring and damper element with a restriction that the overall cushion force acting downwards on the load could not cause the mass to exceed 1g downwards. This allowed the model to simply simulate the load lifting off the cushion. The suspension spring was described by a linear stiffness coefficient. The end-stop buffers were described by non-linear stiffnesses. The suspension damper force-velocity characteristic was included as a two-stage 3^{rd} order polynomial curve fit to the measured damper force-velocity characteristic. Friction forces from the damper and the suspension linkage were modelled as constant forces opposing the motion or as a force just sufficient to prevent motion if the acting force was insufficient to overcome the friction force.

3.2.2 Measurement of component parameters

3.2.2.1 Overview

Describing a seat mathematically in terms of coefficient relating directly to the dynamic properties of the component parts required separate dynamic measurements of each of the components. However, this approach allowed the influence on the seat behaviour of a specific component to be investigated. The following sections describe briefly the measurements used to describe the seat components in terms of parameter values for use in the model. A summary of the parameter values used to describe the two seats can be found in Section 8 and a more detailed description of the measurements used to identify the seat components in terms of coefficient values can be found in Gunston (2000).

3.2.2.2 The cushion

The cushions were preloaded to 500 N and subjected to a random motion band- limited at 1 Hz and 10 Hz. The applied acceleration and transmitted force were measured and converted to estimates of the cushion linear stiffness and damping using the following equations derived from Wei and Griffin (1998).

$$k(w) = -\mathrm{Re}(M(w)) \cdot w^2 \qquad (5)$$

$$c(w) = -\mathrm{Im}(M(w)) \cdot w \qquad (6)$$

where k is the cushion stiffness, c is the cushion damping, and M is the cushion apparent mass. The estimated cushion stiffness, damping and coherency of the earthmover seat cushion are shown in Figure 7. The cushion stiffness varied by less than 10% over this range investigated. The cushion damping showed more variation over the frequency range. In both cases the values at 2 Hz were taken.

3.2.2.3 The suspension linkage and stiffness

The suspension mechanisms were subjected to a quasi-static force-deflection test with the cushion and suspension damper mechanism removed. The suspension linkage force-deflection characteristic for the earthmover seat is shown in Figure 8. The suspension linkage friction was estimated as half the mean difference between the force in compression and extension over the free travel region between the end-stop buffers. The effective vertical suspension spring rate was estimated as the mean gradient over the same region.

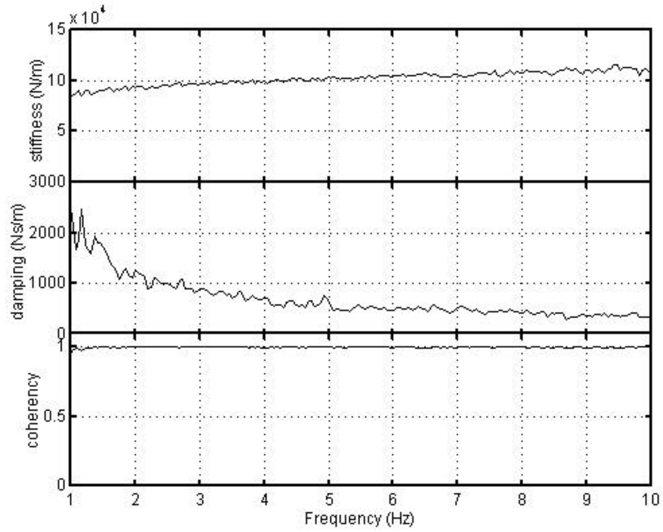

Figure 7 Estimated cushion stiffness and damping

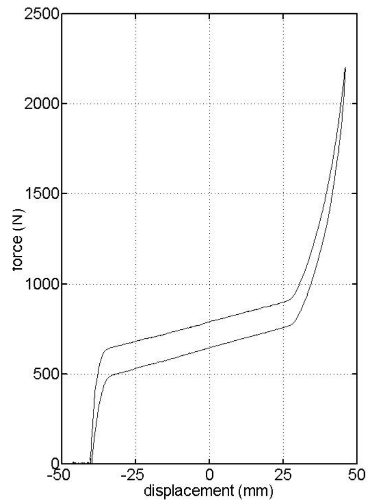

Figure 8 Suspension force-deflection characteristic

3.2.2.4 The suspension damper

The earthmover damper was tested on a commercial damper test rig that extracted the force-velocity characteristic and the friction in compression and extension from the measured damper response to sinusoidal excitations. The industrial truck damper was tested on an alternative apparatus. The force-velocity characteristic and friction values were again extracted from the response to sinusoidal excitations.

The friction value was estimated as the force transmitted by the damper at low velocities (<0.1 ms^{-1}). The force-deflection characteristic was modelled as a two-stage 3rd order polynomial as shown in the following equations. Separate sets of coefficients were used to describe the friction and the force-velocity characteristic in compression and extension. The change in damping force with displacement due to the angled damper mounting used in the earthmover seat was accounted for.

$$F_1 = c_1\dot{z} + c_2\dot{z}^2 + c_3\dot{z}^3 \Big|_{\dot{z} < \dot{z}_1} \tag{7}$$

$$F_2 = c_4(\dot{z} - \dot{z}_1) + c_5(\dot{z} - \dot{z}_1)^2 + c_6(\dot{z} - \dot{z}_1)^3 + c_1\dot{z}_1 + c_2\dot{z}_1^{\,2} + c_3\dot{z}_1^{\,3} \Big|_{\dot{z} \geq \dot{z}_1} \tag{8}$$

$$F_c = F_1 + F_2 \tag{9}$$

where $\dot{z}$ is the relative velocity across the damper along the damper axis, F_c is the damping force and $\dot{z}_1$ is the velocity at which the damper changes between the polynomial described by coefficients c_1, c_2, c_3 and that described by coefficients c_4, c_5, c_6.

3.2.2.5 The end-stop buffers

The end-stop buffers were described in terms of 5^{th} order polynomial functions. The coefficients of these polynomials were determined by applying a least-squares curve fit to the measured buffer force-deflection characteristics.

3.2.3 Optimisation of damper parameters

As mentioned previously, the advantage of describing the seat in terms of individual parameters is that the effect of each component on the seat performance can be determined. The disadvantage of this approach is that a mathematical model and suitable parameter values must be obtained to describe every seat component part that affects the seat dynamic performance. Some of the seat components, such as the suspension damping and friction, were found to be difficult to measure.

Two sets of seat component parameters were used to describe each seat for the present investigation using the ISVR model. The first set was as measured by testing the individual components using the methods described in Gunston (2000). That study demonstrated that the damper coefficients could have a substantial influence on the predicted seat performance.

However, subsequent investigations (to be presented at the 2001 United Kingdom Conference on Human Response to Vibration) cast some doubt on the repeatability of measurements of the suspension damper coefficients, in particular the suspension friction. Repeated measurements of the same damper using different sets of apparatus and different methods resulted in substantially different friction values. The method of mounting the damper in the test rig and any resulting off-axis loads were suspected. Consequently, a simple downhill search algorithm was used to obtain a second set of coefficients for the suspension damper by curve fitting to measured data.

This process involved minimising the root-mean-square (r.m.s.) error between the measured and predicted seat load acceleration time histories using a gain applied to the force-velocity characteristic and a gain applied to the friction coefficients. The friction gain was optimised using a magnitude that did not cause end-stop impacts, and the force-velocity gain was obtained using a motion that caused severe end-stop impacts. The form of test motion as shown in Figure 9 was used in all cases, with a frequency of 2.35 Hz. The magnitudes of these motions are shown in Table 3. Different magnitudes were used for the different seats as the differing seat properties caused end-stop impacts to occur at different magnitudes.

The second set of coefficients was therefore identical to the first, apart from a gain applied to the force-velocity characteristic and a second gain applied to the friction coefficients. These gains are shown in Table 4.

Table 3 Seat base accelerations of the 2.35 Hz motions used to optimise the suspension damping parameters expressed in terms of r.m.s. acceleration and W_k-weighted VDV.

	Motion used to optimise the friction coefficients (no end-stop impacts)		Motion used to optimise the damper force-velocity coefficients (end-stop impacts occurred)	
	r.m.s. accel	VDV	r.m.s. accel	VDV
Earthmover seat	1.82 ms^{-2}	1.62 $ms^{-1.75}$	3.83 ms^{-2}	3.42 $ms^{-1.75}$
Industrial truck seat	0.89 ms^{-2}	0.78 $ms^{-1.75}$	1.84 ms^{-2}	1.63 $ms^{-1.75}$

Table 4 Optimal gains for the suspension damping coefficients as determined by the optimisation process

	Gain applied to the friction coefficients	Gain applied to the damper force-velocity characteristic coefficients.
Earthmover seat	0.61	0.70
Industrial truck seat	1.36	0.85

4 Experimental procedure

4.1 Laboratory seat tests

An earthmover seat and an industrial truck seat were tested in the laboratory at ISVR using a 58 kg rigid seat load. The seats were exposed to three frequencies of transient vibrations derived from vehicle cab floor motions measured in the field on off-road vehicles (Gunston, 1999). The acceleration waveform reproduced at the base of the seat is shown in Figure 9. The frequencies were 2.1 Hz, 2.35 Hz and 3.25 Hz and were chosen as being close to the peak of the power spectrum for the standard simulated vibration seat tests as shown in Table 5.

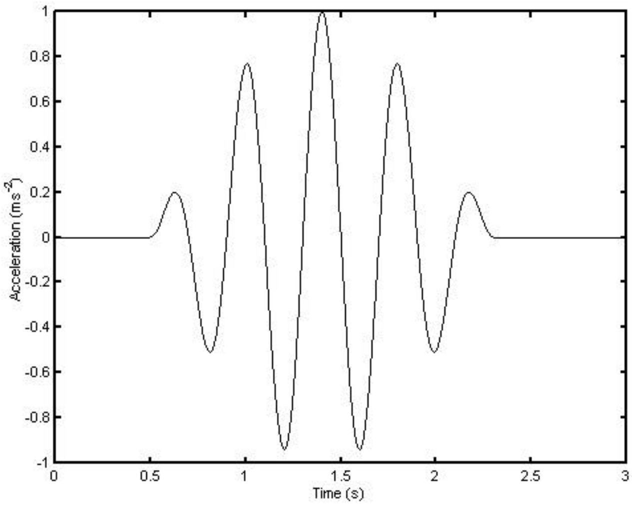

Figure 9 The input motion

Table 5 The approximate frequencies corresponding to the peak acceleration power spectra of standardised vibrations used for suspension seat testing

Approximate frequency of the acceleration power spectrum peak value	**Standard vibration test**	**Intended vehicle**
2.1 Hz	ISO 7096 (2000) EM2	Scraper without suspension
	ISO 7096 (2000) EM3	Wheel loader
	ISO 7096 (2000) EM4	Grader
	ISO 7096 (2000) EM5	Wheel dozer, wheeled soil compactor, backhoe loader
	CEN/TC 231/WG9 (1997) IT4	All terrain industrial trucks
	CEN/TC 231/WG9 (1997) IT3	Industrial trucks above 9000 kg
2.35 Hz	ISO/CD 5007 (1999) Class 2	Agricultural tractor of between 3600 and 6500 kg unballasted mass
3.25 Hz	CEN/TC 231/WG9 (1997) IT2	Industrial trucks between 3500 and 9000 kg

The seats were mounted on an electro-hydraulic shaker capable of ±500 mm peak displacement and ±10 ms^{-2} peak acceleration. The seat index point device, as specified in ISO5353 (1999), was placed on the cushion and was ballasted to 58 kg using rigidly attached steel blocks. The load was placed on the seat at least 5 minutes before any measurements were taken. The driver mass control was adjusted so the mean ride position of the seat suspension was at the mid-point of the available free travel between the end-stop buffers. A 5 Hz ±1 mm sinusoid was used to overcome the suspension friction while adjusting the driver mass control.

The acceleration at the base of the seat and at the base of the load were measured using ENTRAN EGCSY-240D-10 accelerometers and the displacement of the seat suspension relative to the shaker platform was measured using an RDP DCT4000C LVDT. The signals from the transducers were acquired digitally at 512 samples per second using an *HVLab* data acquisition and analysis system via 100 Hz anti-aliasing filters. The acquired signals were low pass filtered at 40 Hz using a 6-pole zero-phase Butterworth filter to attenuate the predominantly 50 Hz measurement noise.

The input motions were generated over the range of magnitudes shown in Table 6 at 20 equally spaced intervals for each frequency. The performance of the seat in response to each motion was characterised using the ratio of the vibration dose value (VDV, see Equation 10) on the seat load to that recorded at the seat base. The VDV was calculated for each motion using the ISO2631 W_k frequency weighting. The frequency weighting was applied using a digital filter including the effects of phase.

$$VDV = \left[\int_{t=0}^{t=T} a_w^4(t)dt\right]^{0.25} \qquad (10)$$

where a_w is the W_k frequency-weighted acceleration.

Table 6 The range of input magnitudes in terms of W_k frequency-weighted VDVs.

Frequency	Earthmover seat		Industrial truck seat	
	Lowest magnitude	**Highest magnitude**	**Lowest magnitude**	**Highest magnitude**
2.1 Hz	0.81 $ms^{-1.75}$	3.30 $ms^{-1.75}$	0.43 $ms^{-1.75}$	1.85 $ms^{-1.75}$
2.35 Hz	0.86 $ms^{-1.75}$	4.20 $ms^{-1.75}$	0.44 $ms^{-1.75}$	1.96 $ms^{-1.75}$
3.25 Hz	1.05 $ms^{-1.75}$	8.05 $ms^{-1.75}$	0.47 $ms^{-1.75}$	5.23 $ms^{-1.75}$

4.2 Simulations

The acceleration time history recorded at the base of the seat was used as the input to the models. The predicted load mass acceleration was used to calculate a predicted VDV for comparison with the laboratory measurements.

Identical predicted and measured SEAT values would indicate that the amount of vibration, in terms of the VDV, was identical but would not necessarily indicate that the model was predicting exactly the same motion for the seat load. The normalised root-mean-square difference between the predicted and measured load mass acceleration, as defined by Equation 11, was also calculated to give an alternative indication of the accuracy of prediction of the acceleration waveform of the load mass.

$$e = \frac{\left[\int_{t=0}^{T}\left(a_{predicted}(t) - a_{measured}(t)\right)^2 dt\right]^{1/2}}{\left[\int_{t=0}^{T} a_{measured}^2(t)dt\right]^{1/2}} \tag{11}$$

5 Results

The VDV on the seat load predicted from the models, compared with the laboratory measurements, is shown for all investigated frequencies of motion in Figure 10 to Figure 15. The corresponding r.m.s. errors between the predicted and measured seat load accelerations are shown in Figure 16to Figure 21.

6 Discussion

The following sections describe the conditions that resulted in differences in behaviour between the models.

6.1 The optimised versus non-optimised ISVR model

The ISVR model using measured values for the damper parameters can be seen to give the poorest results of the three models when compared with the measured results using the earthmover seat. The predictions of the VDV were consistently high in situations without end-stop impacts and consistently low with end-stop impacts, and the r.m.s. error was greater than the other two models with a difference of up to a factor of three at low magnitudes.

The differences between the predicted VDVs when using the industrial truck seat were smaller thanthose with the earthmover seat. The improvements in the r.m.s. error obtained by optimising the damper coefficients were also smaller with the industrial truck seat.

Further investigation of the methods of measuring seat components is required in order to more accurately specify specific components in terms of relevant coefficients. The comparatively good performance of the optimised model, in particular at low magnitudes, indicates that the existing theoretical model is capable of making good predictions of the seat dynamic performance when given a suitable set of coefficients.

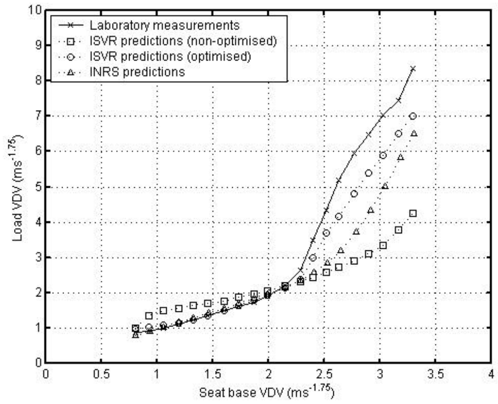

Figure 10 Earthmover seat, 2.1 Hz input

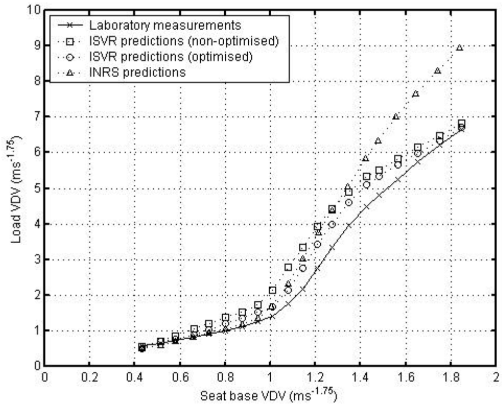

Figure 11 Industrial truck seat, 2.1 Hz input

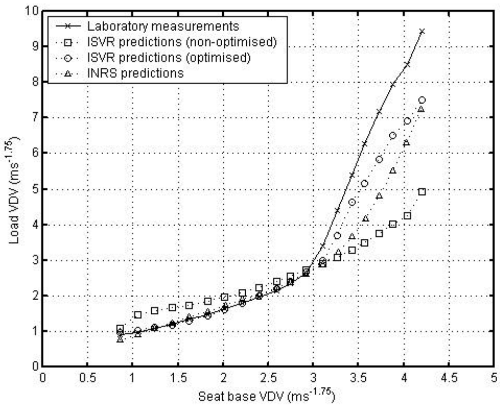

Figure 12 Earthmover seat, 2.35 Hz input

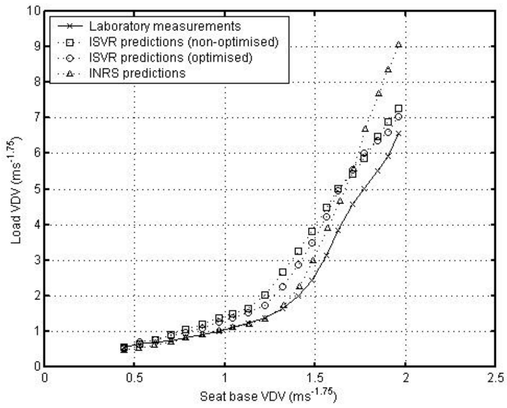

Figure 13 Industrial truck seat, 2.35 Hz input

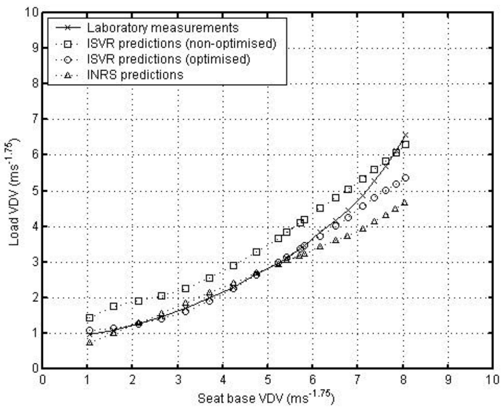

Figure 14 Earthmover seat, 3.25 Hz input

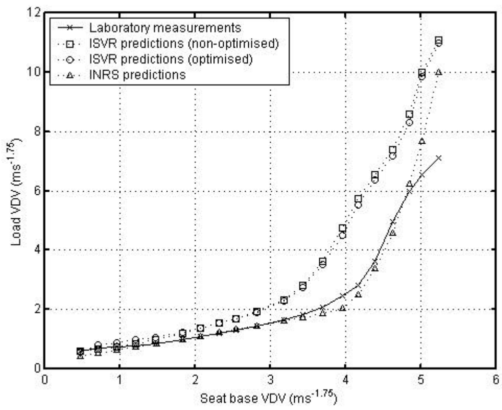

Figure 15 Industrial truck seat, 3.25 Hz input

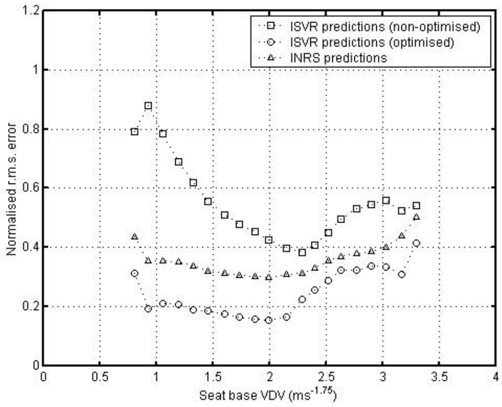

Figure 16 Earthmover seat, 2.1 Hz input

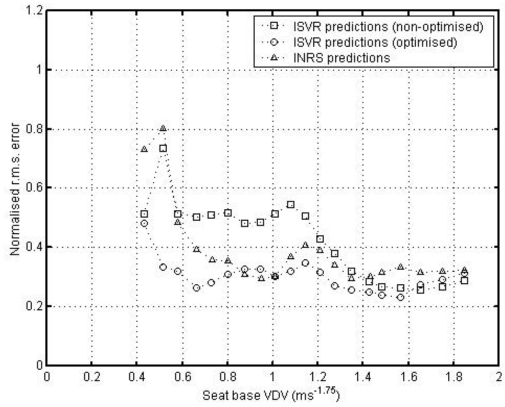

Figure 17 Industrial truck seat, 2.1 Hz input

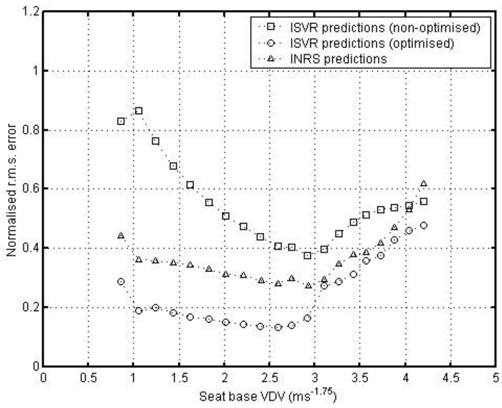

Figure 18 Earthmover seat, 2.35 Hz input

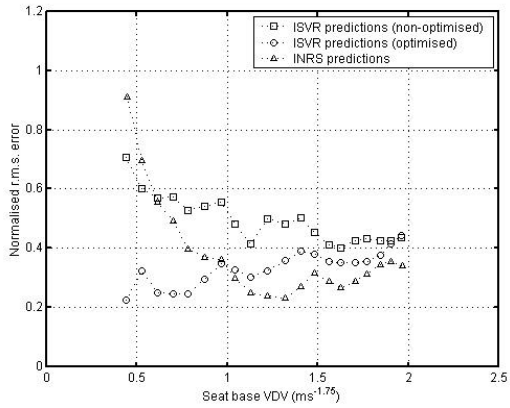

Figure 19 Industrial truck seat, 2.35 Hz input

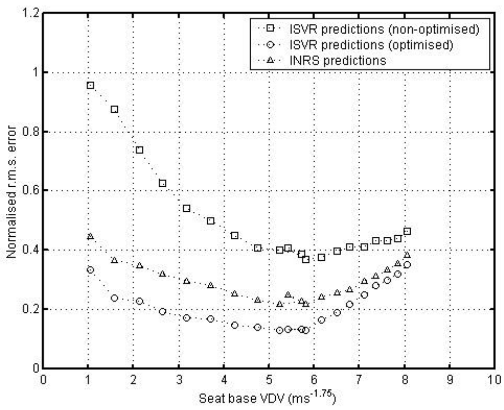

Figure 20 Earthmover seat, 3.25 Hz input

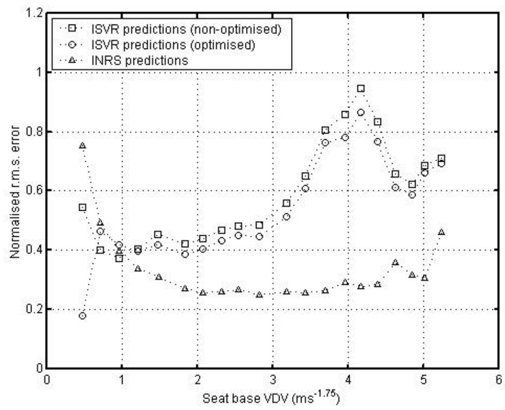

Figure 21 Industrial truck seat, 3.25 Hz input

6.2 Low magnitude performance

The ISVR model resulted in the lowest errors at magnitudes that did not results in end-stop impacts for all frequencies with the earthmover seat, and for all frequencies except for 3.25 Hz with the industrial truck seat. The VDVs predicted by the ISVR and INRS models were similar over this range with the earthmover seat, and the INRS model gave better predictions with the industrial truck seat.

6.3 End-stop impact predictions for the earthmover seat

Both models underestimated the VDV on the earthmover seat in situations involving end-stop impacts, and the r.m.s. error increased with increasing magnitude. Examination of the time histories showed that the models successfully predicted the acceleration due to the bottom end-stop impact, but did not predict a sufficiently severe upwards acceleration as the load returned to the seat after a top-stop impact.

6.4 Severe end-stop impacts with the industrial truck seat

The rate of increase of seat surface VDV with increasing magnitude measured in the laboratory with the industrial truck seat showed a tendency to decrease at high magnitudes. The ISVR model showed this trend while the INRS model did not.

6.5 The industrial truck seat at 3.25 Hz

The ISVR model overestimated the vibration with the industrial truck seat at 3.25 Hz. The INRS model gave better predictions and lower r.m.s. errors at all magnitudes, except for the lowest three magnitudes. The Bouc-Wen suspension model as used by the INRS model appears to be more suitable for modelling the seat suspension in this situation. Optimisation of the ISVR model damper parameters did not result in a large improvement in accuracy.

7 Conclusions

The two alternative models were found to give better performances in different circumstances. Improvements would be expected by refining the cushion models and the cushion-load interface to improve the simulation of top-stop impacts. Improved methods of characterising the seat suspension components (in particular the damper coefficients) would be beneficial to the ISVR model in order to obtain better predictions without optimising any seat component coefficients.

8 Parameters used in the ISVR model

			Earthmover seat	**Industrial truck seat**
Load mass			58 kg	58 kg
Cushion stiffness			92.1 kNm^{-1}	170 kNm^{-1}
Cushion damping			1371 Nsm^{-1}	1250 Nsm^{-1}
Suspension moving mass			27 kg	13.5 kg
Suspension linkage friction			74 N	26 N
Suspension stiffness			4.57 kNm^{-1}	10.4 kNm^{-1}
Suspension damper gas loading stiffness			2.3 kNm^{-1}	N/A
Horizontal distance between damper mounting points at mid ride			150 mm	N/A
Vertical distance between damper mounting points at mid ride			111 mm	N/A
Damper force-velocity characteristic fit coefficients	Compression	c_1	0	0
		c_2	0	0
		c_3	0	0
		c_4	-107	$1.80\text{x}10^{2}$
		c_5	$6.32\text{x}10^{3}$	0
		c_6	0	0
		$\dot{z}_1$	0	0
	Extension	c_1	0	$-3.55\text{x}10^{1}$
		c_2	0	$1.50\text{x}10^{3}$
		c_3	0	0
		c_4	$6.16\text{x}10^{1}$	$1.01\text{x}10^{3}$
		c_5	$1.03\text{x}10^{4}$	$3.49\text{x}10^{3}$
		c_6	0	$1.44\ \text{x}10^{5}$
		$\dot{z}_1$	$4.5\text{x}10^{-2}\ ms^{-1}$	$2.9\text{x}10^{-1}\ ms^{-1}$
Free travel between end-stops			64 mm	50 mm
Damper friction in extension			173 N	30 N
Damper friction in compression			64 N	8 N
Bottom buffer axial force-deflection characteristic fit coefficients where x is the buffer compression		$\cdot x^5$	$1.83\text{x}10^{11}$	$3.20\text{x}10^{12}$
		$\cdot x^4$	$-8.57\text{x}10^{7}$	$-8.04\text{x}10^{10}$
		$\cdot x^3$	$-4.45\text{x}10^{7}$	$8.72\text{x}10^{8}$
		$\cdot x^2$	$1.50\text{x}10^{6}$	$-3.86\text{x}10^{6}$
		$\cdot x$	$7.63\text{x}10^{3}$	$5.42\text{x}10^{4}$
Number of bottom buffers			2	2
Horizontal distance between the ends of the linkage arm at mid ride			295 mm	N/A
Vertical distance between the ends of the linkage arm at mid ride			150 mm	N/A
Top buffer axial force-deflection characteristic fit coefficients where x is the buffer compression		$\cdot x^5$	$5.48\text{x}10^{15}$	0
		$\cdot x^4$	$-2.57\text{x}10^{4}$	$8.2\text{x}10^{11}$
		$\cdot x^3$	$2.60\text{x}10^{3}$	$-6.66\text{x}10^{9}$
		$\cdot x^2$	$3.27\text{x}10^{7}$	$2.17\text{x}10^{7}$
		$\cdot x$	$1.35\text{x}10^{5}$	$3.98\text{x}10^{4}$
Number of top buffers			2	2

9 References

Ahmed OB and Goupillon JF (1997) Predicting the ride vibration of an agricultural tractor. *Journal of Terramechanics, January 1997, vol. 34, no. 1, pp. 1-11(11)*

Baber TT and Wen YK (1981) Random vibration of hysteretic degrading systems. *Journal of Engineering Mechanics Division. ASCE, Vol 107, N° EM6.*

Bouc R (1967) Modèle mathématique d'hystérésis. *Acustica, 24, 16-25.*

CEN/TC 231/WG9: Seating (1997). Draft of proposed industrial truck seat test standard. Committee document number 97/703345.

Gouw G, Rakheja S, Sankar S, Afework Y (1990) Increased Comfort and Safety of Drivers of Off-Highway Vehicles Using Optimal Seat Suspension. *Journal Of Commercial Vehicles, Section 2 - Volume 99, pp 541-548.*

Gunston T (1999) The definition of suitable input motions for testing suspension seat end-stop impact performance. *Human Response to Vibration Conference. Dunton, Essex, England, 22 -24 September 1999.*

Gunston T (2000) An investigation of suspension seat damping using a theoretical model. *Presented at the 35th United Kingdom Group Meeting on Human Response to Vibration, held at the Institute of Sound and Vibration Research, Southampton, England, 13 - 15th September 2000.*

International Organization for Standardization (1997) Mechanical vibration and shock - Evaluation of human exposure to whole-body vibration - Part 1 ; General requirements. International Standard 2631-l.

International Organization for Standardization (1999) Agricultural wheeled tractors - Operator seat - Measurement of transmitted vibration. *Draft international standard ISO/CD 5007.*

International Organization for Standardization (1999) Earth moving machinery, and tractors for agriculture and forestry - Seat index point. International standard ISO5353.

International Organization for Standardization (2000) Earth moving machinery - laboratory evaluation of operator seat vibration. *International standard ISO7096.*

Moré JJ (1977) The Levenberg-Marquardt Algorithm: Implementation and Theory. *Numerical Analysis, ed. G.A. Watson, Lecture Notes in Mathematics 630, Springer Verlag, pp. 105-l 16.*

Nelder JA and Mead R (1965) A Simplex Method for Function Minimization. *Computer Journal, Vol 7, pp. 308-313.*

Rakheja S, Afework Y and Sankar S (1994) An Analytical and Experimental Investigation of the Driver-Seat-Suspension System. *Vehicle System Dynamics, 23 (1994), pp. 501-524*

Rakheja S, Ahmed AKW, Sankar S and Bhat RB (1987) Ride Vibration Levels At The Driver-Seat Interface. *Report prepared by the Concave Research Centre,* Department of Mechanical Engineering, Concordia University, Montreal, Quebec

Ranganathan R and Sriram K (1994) Development of a PC-Based Software for Analysis of Off-Road Vehicle Seat Suspensions. *International Off-Highway & Powerplant Congress & Exposition Milwaukee, Wisconsin September 12-14,1994*

Rebelle J (2000) Development of a numerical model of seat suspensions to optimise the end-stop buffers. *Presented at the 35th United Kingdom Group Meeting on Human Response to Vibration, held at the Institute of Sound and Vibration Research, Southampton, England, 13 - 15th September 2000.*

Tewari VK and Prasad N (1999) Three-DOF modelling of tractor seat-operator system. *Journal of Terramechanics, October 1999, vol. 36, no. 4, pp. 207-219(13)*

Wei L and Griffin MJ (1998) The prediction of seat transmissibility from measures of seat impedance. *Journal of Sound and Vibration 214 (1) pp.121-137*

Wen YK (1976) Method for random vibration of hysteresis systems. *Journal of Engineering Mechanics Division. Proceeding ASCE, Vol 102, No EM2, 249-265.*

Wu X and Griffin MJ (1995) Simulation study of factors influencing the severity of suspension seat end-stop impacts. *The United Kingdom Informal Group Meeting on Human Response to Vibration, Silsoe, 19_21 September.*